Manchester Metropolitan University

TITLE: Titania coating of mesoporous silica nanoparticles for improved biocompatibility and drug release within blood vessels

Short running title: Titania coated mesoporous silica nanoparticles for slow drug release in vessels

Authors: Asima FAROOQ[1], Ali SHUKUR[1], Cai ASTLEY[1], Lubomira TOSHEVA[2], Peter KELLY [2], Debra WHITEHEAD [2*], May AZZAWI [1*]

1, Cardiovascular Research Group, School of Healthcare Science, Faculty of Science and Engineering, Manchester Metropolitan University, Manchester, M1 5GD, UK.

2, Advanced Materials and Surface Engineering Research Centre, Faculty of Science and Engineering, Manchester Metropolitan University, Manchester, M1 5GD, UK.

Corresponding authors:

* Dr. May Azzawi, Tel +44 0161 247 3332, Email m.azzawi@mmu.ac.uk; Dr. Debra Whitehead, Tel +44 161 247 3341, Email d.whitehead@mmu.ac.uk; Faculty of Science and Engineering, Manchester Metropolitan University, Manchester M1 5GD, UK.

Word count (including references and figure captions) = 7,201

ABSTRACT

Blood vessel disease is a major contributor to cardiovascular morbidity and mortality and is hallmarked by dysfunction of the lining endothelial cells (ECs). These cells play a significant role in vascular homeostasis, through the release of mediators to control vessel diameter, hence tissue perfusion. Mesoporous silica nanoparticles (MSNs) can be used as potential drug delivery platforms for vasodilator drugs. Here, using an *ex vivo* model of vascular function, we examine the use of titania coating for improved biocompatibility and release dynamics of MSN loaded sodium nitroprusside (SNP). MSNs (95 ± 23 nm diameter; pore size 2.7 nm) were synthesised and fully characterised. They were loaded with SNP and coated with titania (TiO_2), using the magnetron sputtering technique. Pre-constricted aortic vessels were exposed to drug loaded MSNs (at 1.96×10^{12} MSN mL^{-1}) and the time course of vessel dilation observed, in real time. Exposure of viable vessels to MSNs lead to their internalization into the cytoplasm of ECs, while TiMSNs were also observed in the elastic lamina and smooth muscle cell layers. We demonstrate that titania coating of MSNs significantly improves their biocompatibility and alters the dynamics of drug release. A slow and more sustained relaxation was evident after uptake of TiMSN-SNP, in comparison to uncoated MSN-SNP (rate of dilation was 0.08% per min over a 2.5 h period). The use of titania coated MSNs for drug delivery to the vasculature may be an attractive strategy for therapeutic clinical intervention in cardiovascular disease.

STATEMENT OF SIGNIFICANCE

Cardiovascular disease is a major cause of mortality and morbidity worldwide, with a total global cost of over $918 billion, by 2030. Mesoporous silica nanoparticles (MSNs) have great potential for the delivery of drugs that can treat vessel disease. This paper provides the first description for the use of titania coated MSNs with increased vascular penetration, for the delivery of vasodilator drugs, without compromising overall vessel function. We demonstrate

that titania coating of MSNs significantly improves their biocompatibility and uptake within aortic blood vessels and furthermore, enables a slower and more sustained release of the vasodilator drug, sodium nitroprusside within the vessel, thus making them an attractive strategy for the treatment of vascular disease.

Keywords: mesoporous silica nanoparticles; titania; vascular; dilation; artery

1. INTRODUCTION

Blood vessel disease is a major contributor to cardiovascular disease (CVD) mortality and morbidity, with predicted medical costs projected to reach $918 billion by 2030 [1]. An early predictor and hallmark of CVD is dysfunction of the lining endothelial cells (ECs) [2]. These cells play a significant role in vascular homeostasis, through the release of mediators, to control vessel diameter and prevent atherogenesis [3], particularly relevant for small vessels which control over 50% of blood perfusion into tissues [4]. Hence, there is an urgent need for early therapeutic intervention strategies to preserve and restore vessel health. We have previously demonstrated the uptake of nanomaterials by ECs [5, 6], including mesoporous silica nanoparticles (MSNs), and their highlighted potential use as drug delivery platforms for vasodilator drugs [7]. In particular, MSNs hold great promise as drug delivery vehicles [8, 9]. They can be synthesised with a narrow particle size distribution and a regular pore structure that can accommodate guest molecules, while the exterior surface can be functionalised to allow targeted drug delivery [10, 11]. Manipulation of the synthesis conditions and reactant concentrations allows easy tailoring of small diameters that are able to enter cells including non-phagocytic cells, such as ECs that line blood vessels. ECs are thus an easily accessible target for therapeutic intervention using nanoparticles, when injected intravenously. This can be especially attractive for targeted delivery of vasodilator drugs for subjects with CVD. However, despite such potential uses, silica nanoparticles have previously been shown to affect vascular function, depending on their surface charge, dye

doping and size [5, 12, 13]. Silica nanoparticles (SiNPs) can generate reactive oxygen species (ROS), such as hydroxyl radical ($^{\bullet}$OH), superoxide anion ($O_2^{-\bullet}$) and hydrogen peroxide (H_2O_2), causing an imbalance between the oxidant and antioxidant processes, thus leading to intracellular oxidative stress [14]. Furthermore, increased ROS generation can quench nitric oxide leading to attenuated dilator responses. In contrast, nanoparticles of certain material composition, such as ceria, have antioxidant properties that protect cells by scavenging hydrogen peroxide or superoxide leading to improved dilator function [6].

Titania (titanium dioxide; TiO_2) has attracted a great deal of interest due to its physicochemical, electrical, and optical performance characteristics, as well as its photocatalytic and anticorrosion properties [15, 16]. Recently, TiO_2 nanotubes have been used as reversible oxygen scavengers via an electrochemical approach. Interestingly, the authors showed that the re-uptake of oxygen is rapid when the electrochemical reduction occurs under basic conditions, while under acidic conditions the oxygen re-uptake is approximately three times orders slower [17]. Wu and colleagues assessed the biocompatibility of amorphous titania nanoparticles synthesised by the sol-gel technique and commercially available P25 consisting of crystalline anatase titania on human breast cancer cells, demonstrating that amorphous titania had lower toxicity and excellent biocompatibility (LC50 400 mg mL^{-1}) [18]. Hence, surface coating with titania may improve biocompatibility of the MSNs.

In the present study, we synthesised and fully characterised titania coated MSNs and examined the effect of coating on the biocompatibility and release dynamics of MSNs loaded with the endothelial independent dilator, sodium nitroprusside (SNP) as a model drug. Vessel uptake and drug release was examined, in real time, using an *ex vivo* model of vascular function. The results demonstrate that by titania coating the MSNs surface, they have less detrimental influence on vasodilator responses, while demonstrating increased penetrability within the vessel wall allowing for a slower and more sustained relaxation response of aortic vessels.

2. Materials and methods

2.1. Materials

Tetraethyl orthosilicate (TEOS), hexadecyltrimethyammonium bromide (CTAB), anhydrous dimethylformamide (DMF), sodium hydroxide (NaOH), hydrochloric acid (HCl, 37 %), methanol (MeOH), acetylcholine chloride (ACh) and sodium nitroprusside (SNP) were purchased from Sigma-Aldrich. Salt solutions were prepared using sodium chloride (NaCl), potassium chloride (KCl), magnesium sulphate heptahydrate ($MgSO_4 \cdot 7H_2O$), potassium phosphate monobasic (KH_2PO_4), calcium chloride ($CaCl_2 \cdot 2H_2O$), ethylenediaminetetraacetic acid dipotassium salt dihydrate ($K_2EDTA \cdot 2H_2O$) purchased from Fisher-Scientific. Physiological Salt Solution (PSS) and high potassium PSS (KPSS; 60 mM KCL) were prepared as previously described [13].

2.2. Synthesis and drug loading of mesoporous silica nanoparticles

MSNs were synthesised using the surfactant template directed method followed by removal of the CTAB template [19]. Dried MSNs were drug loaded by mixing in a solution of SNP (1 g MSNs dispersed in 50 mL 1×10^{-4} M drug solution in MeOH) for 48 h. The drug loaded particles were collected by centrifugation, dried at 50 °C overnight and stored in a glass vial wrapped in aluminium foil; the drug-loaded MSN were assigned the name MSN-SNP. The iron concentration in the supernatant originating from the SNP drug was quantified by inductively coupled plasma atomic emission spectroscopy (ICP-AES) and the quantity of drug loading was calculated.

2.3. Coating mesoporous silica nanoparticles with titania

Titania was deposited onto MSNs and drug loaded MSN-SNP using the physical vapour deposition technique of reactive magnetron sputtering [20]. A Teer Coatings UDP 450 coating system fitted with a custom built oscillating mechanism in the coating chamber was utilised [21]. MSN powders (10 g) were added to a 250 mm diameter bowl that was vibrated by the oscillating mechanism and positioned under the magnetron. The vibrating motion allows exposure of all the surfaces of the MSN to the coating flux from the magnetron. Titania was deposited for 1 hr using two titanium metal plate targets (99.5% purity), argon (99.998% purity) as the working gas and oxygen (99.5% purity) as the reactive gas. The working pressure was 0.1 Pa. Advanced Energy Pinnacle Plus pulsed DC power supplies were used to power the titanium target. The power supply was set to 1000 W per target, pulse frequency of 100 kHz and a pulse off time of 4 μs, giving a duty cycle when the magnetron operates of 60%. At this power, the target voltage is approximately -300 V and the current is approximately 3.3 A. The amount of oxygen was controlled using an optical emission monitor, using conditions known to produce stoichiometric TiO_2 [22]. The final products were stored as a powder in a foil covered glass vial and assigned names of TiMSN (titania coated mesoporous silica nanoparticles) and TiMSN-SNP (titania coated SNP loaded mesoporous silica nanoparticles).

2.4. Drug release from titania coated mesoporous silica nanoparticles, in vitro

The MSN-SNP or TiMSN-SNP drug release rates were determined using the dialysis method as previously described [7]. In brief, MSN-SNP or TiMSN-SNP (0.128 g) were dispersed in KPSS (4 mL) and placed in the dialysis tubing and sealed. The dialysis tube was placed in KPSS (11 mL) and the drug release was determined by measuring the concentration of iron in the external solution over time by ICP-AES. The release profile of SNP released from the MSN was expressed as the ratio of cumulative drug release to initial drug loading versus time (Eq. 1):

$$\text{percentage of drug release} = \frac{M_t}{M_0} \times 100 \qquad \text{(Eq. 1)}$$

where M_t is the cumulative amount of drug released at time t and M_0 is the amount of drug loaded in the MSNs.

2.5. Characterisation of mesoporous silica nanoparticles

The MSNs, TiMSNs and corresponding drug loaded particle sizes and morphology were examined using scanning electron microscopy (SEM, JEOL 5600LV SEM) and transmission electron microscopy (TEM, Philips Technai™ 12 Biotwin TEM). The MSNs and TiMSNs hydrodynamic size and zeta potential were determined by dynamic light scattering (DLS) and laser Doppler velocimetry, respectively (Malvern Zetasizer nano ZS instrument, UK). DLS measurements were performed for MSNs suspended in distilled water and in KPSS solution. The hydrodynamic size was measured by an infra-red light passing through the sample and any resulting scattered light was detected. Nitrogen adsorption isotherms at -196 °C were measured with a Micromeritics ASAP 2020 instrument. Samples were degassed at 90 °C overnight prior to analysis. The surface areas were calculated using the Brunauer-Emmett-Teller (BET) method and Barrett-Joyner-Halenda (BJH) pore size distributions were determined from the desorption branches of the isotherms. Attenuated Total Reflectance Infrared Fourier-transform Infrared Spectroscopy analysis (ATR) was used for confirmation of template removal (Nicolet Avatar 360 ATR-FTIR). Semi-quantitative chemical analysis was performed on MSNs by energy-dispersive X-ray spectroscopy (EDS) using a detector from Oxford Instruments to confirm the presence of titania coating. X-ray diffraction (XRD; PANalytical X'Pert X-ray diffractometer employing Cu Kα radiation (40 kV and 30 mA) and a PIXcell detector) was used to determine crystal structure of the materials produced and confirm the ordered pore structure of the MSNs.

2.6. Detection of nanoparticle reactive oxygen species (ROS) generation

The generation of reactive oxygen species by nanoparticles in solution was detected using a dichlorofluorescein (DCF) assay as previously described [23]. Briefly, a 1 mM stock solution was prepared by dissolving DCFH-DA powder (Sigma, UK) in MeOH. The solution was deacetylated using NaOH and kept in darkness at room temperature for 30 min. Stock solution was diluted 1:100 with sodium phosphate buffer to form a working solution. Nanoparticles (10 mg) were dissolved in 200 µL of working solution and sonicated for 15 min. Solutions were transferred into a 96-well plate. Horseradish peroxidase (HRP) was added to each well to initiate the catalytic reaction. Fluorescence kinetics was analysed using a plate reader (Synergy, HT) every minute for 20 min (Exc. 485 nm; Em. 530 nm). Solid non-porous SiNPs were used as a control. These were synthesised and characterised as described in the supplementary material. The working solution, in the absence of HRP, was used as a negative control.

2.7. Vascular functional studies

Aortic vessels were carefully dissected and isolated from male Wistar rats (150-250 g weight; n=26 animals; one vessel from each animal), which were humanly killed by stunning followed by cervical dislocation following institutional approval and in accordance with guidelines issued by the European Commission Directive 86/609/EEC. The vessels (3-4 mm aortic rings) were mounted in an organ bath system filled with gassed PSS solution (95 %O_2: 5% CO_2, 35 $^{\circ}$C) as previously described [6]. In the first set of experiments, release of the SNP drug from the nanoparticles was assessed over a 3 h period. The effect of the MSN-SNP and TiMSN-SNP was examined by the addition of 1.96×10^{12} MSN mL^{-1} (calculated as detailed in the supplementary material) to preconstricted vessels, and incubating within the organ bath for 10 min at 35 $^{\circ}$C. Vessels were then washed in KPSS and tension values

(hence degree of dilation/constriction) constantly monitored in real time, using labchart software (Powerlab Ltd).

In a separate set of experiments, vasodilator responses to endothelium-dependent and independent agonists were examined by firstly pre-constricting vessels in high potassium solution and then adding cumulative doses of acetylcholine (ACh; 0.01-100 μM) or SNP (0.01-10 μM), before and after incubation with the range of nanoparticles.

The uptake and localisation of nanoparticles within the tissue was examined after fixing and sectioning aortic vessels using TEM. Vessels were fixed immediately after the functional studies, using 2.5 % glutaraldehyde and samples observed using a Tecnai 12 Biotwin TEM at 80 kV as previously described [13]. The relative amount of nanoparticle uptake by the vessels was quantified by measurement of silica concentration using ICP-AES. Briefly, vessels were weighed and incubated with nanoparticles (1.96×10^{12} MSN mL^{-1} in PSS) for 10 min and then rinsed to remove any nanoparticles not taken up. Vessels were then digested by placing into a glass vial with high purity (70%) nitric acid (1 mL) and heated in an oil bath at 80°C for 2 h. The solution was made up to 5 mL in a volumetric flask with Millipore distilled water and analysed. A standard curve was used to quantify the amount of silica in the tissues, using standards (Sigma, Poole, UK), in the same background solution as that of the tissue solutions. The limit of Si quantification was 50 ng mL^{-1}. The silica concentrations were used to calculate the percentage uptake.

2.8. Statistical analysis

Data are expressed as mean ± standard error of mean with 'n' representing the number of vessels. Dilator responses are expressed as percent relaxation. The maximum agonist effect (E_{max}) and concentration inducing 50% of E_{max} (EC_{50}) were determined from each concentration response curve and pD_2 was calculated as the –log (EC_{50}). E_{max} and pD_2 values were calculated using the GraphPad Prism Software 7. Concentration response

curves were assessed using statistical package for the social sciences (SPSS; version 19).

The difference between groups at a given concentration was tested by one-way analysis of

variance (ANOVA) with Bonferroni corrections; or Dunnetts multiple comparison test for the

ROS assay. P<0.05 were considered statistically significant [13].

3. RESULTS

3.1. Characterisation of mesoporous silica nanoparticles

The synthesised MSNs had a relatively narrow size distribution with an average

diameter of 95±23 nm with mostly spherical morphology with some elongation (Fig. 1A). After

soaking in SNP the particles had a similar appearance with the surface looking slightly

rougher (Fig. 1B). Small crystallites can be observed on the surface of TiMSNs (Fig. 1C) and

TiMSN-SNP (Fig. 1D). The TEM image showed that the MSNs (Fig. 1E) had regular, parallel-

aligned pore channels confirming the presence of uniform mesopores. The TiMSN had a

rough surface with the individual titania nanoparticles on the surface of the MSN with a size

of ca. 5 nm (Fig. 1F). The average diameter increased to 156±19 nm with an estimated 30.5

nm titania shell thickness surrounding the MSNs. The EDS of MSN confirms the presence of

silica (Fig. 1G). The TiMSN contain both silica and titanium (Fig. 1H). The XRD analysis

showed low angle peaks at 2.8 degrees attributed to [100] reflection from hexagonally

packed mesopores for both MSN and TiMSN and confirmed the preservation of the pore

structure after magnetron sputtering and drug loading (Fig. 2A). As expected, no crystalline

titania peaks (anatase or rutile) were observed. Previous studies have shown that coatings

deposited using this technique are amorphous in the as-deposited state and require post-

deposition annealing to develop crystalline structures [21]. ATR was used for confirmation of

template removal (Fig. 2B). The characteristic organic surfactant CTAB peaks at 2853 cm^{-1}

and 2923 cm^{-1} were diminished after acid extraction. Nitrogen adsorption-isotherms of MSN, TiMSN and corresponding SNP-loaded samples are shown in Fig. 2C. The isotherm of MSN is typical for MCM-41-type materials with a steep step below p/p$_0$ of 0.4 corresponding to capillary condensation in the uniform pores. The isotherm is in agreement with the TEM and XRD results confirming the regularity of the pores in this sample. An average pore size of 2.7 nm was determined from the BJH desorption pore-size distribution (Fig. 2C, inset). The pore-size distribution also indicated the presence of larger pores, which could be related to inter-particle textural porosity. The regularity of the pores was inferior in TiMSN; the step corresponding to the uniform pores was less pronounced and the corresponding peak in the pore-size distribution plot was lower and broader. This result is also in agreement with the TEM images. Nevertheless, the BET surface areas of the two samples were similar, 1071 m^2 g^{-1} for MSN and 1194 m^2 g^{-1} for TiMSN. The drug-loaded samples showed similar isotherms and similar pore-size distributions (Fig. 2C). The BET surface areas of these samples were 383 m^2 g^{-1} for MSN-SNP and 426 m^2 g^{-1} for TiMSN-SNP, respectively. The disappearance of the steep step below 0.4 relative pressure indicated that the drug was adsorbed within the uniform mesopores. It is worth noting that the Ti coating of the latter sample was performed on the MSN-SNP sample. The presence of SNP in the uniform pores may explain the similarity in the MSN-SNP and TiMSN-SNP isotherms. In the case of TiMSN, an 'open-pore' MSN sample was used for Ti deposition, which could be the reason for the differences observed in the corresponding isotherms.

The hydrodynamic diameters of the synthesised MSNs show an overall increase in size when compared to the particle sizes observed by electron microscopy (Table 1). A further increase in hydrodynamic diameter was evident when uncoated MSNs were dispersed in KPSS (188.8 nm vs 247.3 nm in water and KPSS respectively). The titania coating of the MSNs caused the size to increase, with some aggregation as evidenced by the presence of the second peak. The drug loaded TiMSNs remained stable after being placed in KPSS as the hydrodynamic diameter remained similar (250.5 nm vs 313.1 nm in water and KPSS

respectively). It is noteworthy that the concentration of NPs held in the solution for DLS analysis was 0.02%, while for the organ bath experiment the concentration was far smaller and consequently less likely to aggregate. The Zeta potential values for the MSNs and TiMSNs demonstrates that they were stable, even after drug loading (Table 1).

3.2. Detection of nanoparticle reactive oxygen species generation

The generation of ROS by the synthesised MSNs was assessed by measuring the relative degree of fluorescence generated by the nanoparticles in solution, using the DCF assay. There was a significant reduction in fluorescence by all the MSNs, in comparison to the non-porous SiNPs ($p<0.001$). In addition, although there was a reduction in the degree of fluorescence by the titania coated MSNs, in comparison to uncoated MSNs, this was not significant (Figure 2D).

3.3. Loading and release of sodium nitroprusside from mesoporous nanoparticles

The drug loading of the MSN was determined to be 89.1% from the ICP-AES data indicating good drug adsorption efficiency within the pore structure. The SNP release profile for MSN-SNP and TiMSN-SNP was plotted using the cumulative concentration determined from the ICP_AES (Fig. 3A). The time course of SNP release demonstrated that there is a rapid initial release from MSN-SNP the first 10 min, whilst there was a lower concentration of released SNP and slower initial release for TiMSN-SNP. The initial steep increase is expected due to the large concentration gradient and some desorption from the particle exterior surface. The TiMSN-SNP shows a retardation of the release due to the SNP percolating past the titania surface coating. From 30 min to 240 min there is a shallow gradient for both types of particles in the graph indicating slow release.

3.4. Analysis of Release Data

The description of release profiles can analysed using different release models [24].

Our data were evaluated according to the following equations:

1) First-order model $\qquad ln M_t = ln M + k_1 \times t$ (Eq. 2):

2) Higuchi model $\qquad M_t = k_H \times t^{\frac{1}{2}}$ $\qquad$ (Eq. 3):

3) Korsmeyer-Peppas model $\qquad \frac{M_t}{M_\infty} = k_{KP} \times t^n$ $\qquad$ (Eq. 4):

where M_t is the cumulative amount of drug released at time t, M is the initial amount of drug

present in the solution, k_1 is the first-order release constant, and k_H is the Higuchi release

constant. For the Higuchi model, the following assumptions are made: (i) the drug

concentration in the MSN is initially much higher than the solubility of the drug; (ii) diffusion

takes place in a single direction, i.e. perpendicular from MSN pore entrance surface; (iii) the

MSN pore is much larger than the size of the SNP molecules; (iv) the swelling and

dissolution of the MSN is negligible; (v) the diffusivity of the SNP is constant; (vi) and perfect

sink conditions are attained in the release environment. A sink condition is such that the total

dissolution of the SNP molecule in solution yields a resulting concentration that is much

lower than that of saturation. M_t / M_∞ is a fraction of drug released at time t, k_{KP} is the

Korsmeyer-Peppas release constant, and n is the diffusional release exponent indicative of

the release mechanism. When $n < 0.5$ then the drug release mechanism follows Fickian

diffusion model [25] and if $0.5 < n < 0.89$ then the release mechanism follows an anomalous

diffusion model [26]. However, if $n = 0.5$ then the release mechanism follows Higuchi kinetic

model [25].

The kinetics of the delivery was studied to determine the release mechanism by

fitting the curves of cumulative released SNP % as a function of time to three different

mathematical models. Assuming that a simple diffusion process occurs, the kinetics of SNP

release from the pores of the MSN could be explained by the Higuchi model which is based

on Fick's Law where the release occurs by the diffusion of drugs within the delivery system. In this case, the cumulative released amount of the drug is proportional at square root of time. Under some experimental situations the release mechanism can deviate from Fickian diffusion, following an anomalous transport (non-Fickian release). In these cases, a more generic equation can be used. According to the Korsmeyer-Peppas model, where exponential drug release relates to elapsed time, the n value could be obtained from the slope of the straight line of log cumulative amount of drug release (%) versus log time. The release constants were calculated from the slope of the appropriate plots, and regression coefficient (R^2) by linear regression analysis. The correlation coefficient (R^2) was used as an indicator of the best fitting, for each of the considered models. The model with the highest co-efficient of determination (R^2) indicates the most appropriate model for the release profile data [27]. The release regression values (correlation coefficient values) are shown in Table 2

A good linear fit was observed for MSN-SNP and TiMSN-SNP for both Higuchi and Korsmeyer-Peppas models (Fig. 3), indicating that the delivery of SNP from the pores is a diffusive process. The best fit with R^2 is the values from the Higuchi plot (0.9722 for MSN-SNP and 0.9553 for TiMSN-SNP), thus the drug release of SNP was proportional to the square root of time. The SNP drug gradually dissolves into surrounding fluid and then the drug slowly diffuses from the mesoporous silica capillary channels in accordance with a dissolution-filling approach. The rate of release for the MSN-SNP was higher than the TiMSN-SNP as indicated by the K_H values of 3.715 and 2.434 % $min^{0.5}$, respectively.

3.5. Detection of mesoporous silica nanoparticles within vascular tissue

Exposure of aortic vessels to the nanoparticles led to their rapid uptake. MSNs and TiMSNs were internalised into the cytoplasm of the endothelial cells lining aortic vessels (Fig.4A, B). MSNs identified freely within the cytoplasm and were surrounded by a transparent membrane structure suggesting their uptake via endocytosis. The titania coated particles were also observed in the smooth muscle cells and the elastic lamina layer (Fig. 4C, D). None were observed in the nuclei of cells or adventitial layer. The amount of nanoparticles taken up into the tissue was quantified by ICP-AES, and found to be 13% and 14% for TiMSN and TiMSN-SNP; 10% and 11% for MSN and MSN-SNP respectively, after 10 min incubation at 35 $^\circ$C.

3.6. Sodium nitroprusside release from mesoporous silica nanoparticles, *ex vivo*

Pre-constricted aortic rings were exposed to MSN-SNP and TiMSN-SNP in the organ-bath system and incubated for 10 min before washing off (Fig. 4E). The time course of vessel dilation could be observed in real time by monitoring the change in vessel tension. There was an initial rapid relaxation response (phase 1 at 0-10 min) that is likely to be due to release of the adsorbed SNP on the surface. After washout, vessels constricted rapidly and this is likely to be due to removal of the free SNP from the KPSS solution (Phase 2 at 10-30 min). Thereafter, vessels dilated slowly (phase 3 at 30-70 min) likely due to release of the SNP from within the MSNs that are taken up by the vessel. This was calculated from the slope to be 12.36% for the TiMSN-SNP. The final phase at 70-180 min is a slow sustained minimal dilation for the TiMSN-SNP. Although the magnitude of the dilator response was significantly higher after incubation in MSN-SNP (maximal at 75.46% vs 55.73% after 1 h incubation in MSN-SNP and TiMSN-SNP respectively), likely due to release of surface adsorbed SNP from the MSN-SNP, there was a continued slow sustained dilator response in the Ti-MSN-SNP incubated vessels. The overall rate of dilation, due to TiMSN-SNP over a 2.5 h period was 0.08% per min. No relaxation was evident after the washout period for the MSN-SNPs. Any minimal

dilation/constriction is dictated by the amount of SNP released in relation to the overall KPSS concentration in the water bath.

3.7. Influence of mesoporous nanoparticles on vasodilator responses of aortic vessels

All vessels constricted to high potassium solution (60 mM KCl). All pre-constricted vessels dilated to the endothelial-dependent agonist (ACh) and the endothelial-independent agonist (SNP) in a dose dependent manner. There was a significant rightward shift in the concentration-response curve (Fig.4F) and reduced maximal dilation to ACh following MSN incubation (E_{max} 38.52 ± 1.95%; pD_2 3.32 ± 4.09 µM; n=5; vs E_{max} 52.40 ± 1.05%; pD_2 0.52 ± 0.31 µM; n=4, for MSN and control responses respectively, $p<0.05$). Incubation in TiMSN led to a significant improvement in dilator responses as compared to MSN alone with no effect on the E_{max} and pD_2 (E_{max} 40.60 ± 0.55%; pD_2 0.51 ± 0.18 µM; n=4; vs E_{max} 52.40 ± 1.05%; pD_2 0.52 ± 0.31 µM; n=4, for TiMSN and control responses, respectively).

Vessel incubation in MSN or TiMSN had no overall influence on endothelial independent (SNP) dilator responses. However, there was a significant improvement at 0.1 µM concentration only, after incubation in TiMSN (figure 4G).

4. Discussion

The key findings of this study are that coating of MSNs with titania, 1) enables a slow and more sustained release of payload, and 2) increases their biocompatibility and uptake within blood vessels. We utilised SNP as a vasodilator drug and an *ex vivo* model of vascular function to demonstrate blood vessel dilation, in real time.

Using modelling, we show a slower rate of drug release from the TiMSN-SNP than from MSN-SNP. Furthermore, we demonstrate that the release of SNP from the pores of MSNs follows Fickian diffusion (for both coated and uncoated nanoparticles), where drug release is proportional to the square root of time, according to the Higuchi model. Rapid uptake of MSNs by the vessel wall, led to vessel relaxation that was significantly greater after uptake of MSN-SNP than TiMSN-SNP, due to the higher rate of release of surface adsorbed SNP from the MSN-SNP nanoparticles. In contrast, the slow and sustained dilation evident after uptake of TiMSN-SNP, may be due to their increased penetrability into the elastic lamina and smooth muscle cell layers, where the local release of nitric oxide acted directly on smooth muscle cells to induce dilation. Previous studies have demonstrated that titania nanoparticles have a high affinity towards phosphate species [18] and are able to penetrate the phospholipid bilayer, rather than adsorb on the cell membrane surface, which may account for our observation of increased uptake of TiMSNs into the vessel wall [28]. Additionally, titania has catalytic and oxygen scavenging properties due to an interstitial oxygen defect [15]. However, some studies have demonstrated that the limiting step of oxygen uptake by metal oxides is dependent on thermally activated diffusion of bulk oxygen vacancies (VO) and that these vacancies are removed by adsorbed oxygen [29, 30]. Recent research describes the major defect transport mechanism that occur in metal oxides, in particular TiO_2, to be VO and metal interstitials [17, 30]. The lower reduction levels found in TiO_2 at low pH leading to failure in oxygen uptake maybe caused by hydrogen evolution competing with oxygen extraction. Thus, protons intercalation occurs instead of the occurrence of oxygen extraction within TiO_2 lattice [17]. Shkrob and colleagues demonstrated that polyhydroxylated compounds are readily oxidised by holes scavengers contained within TiO_2. The scavenging efficiency is known to increase in accordance to anchoring hydroxyl groups [32]. Titania's catalytic activity can cause cellular reactivity and interactions with enzymes including extracellular metalloproteinases [16; 33]. This may also explain the increased penetrability of titania coated nanoparticles through the elastic lamina.

We demonstrate that titania coating of MSNs improves biocompatibility and prevents their detrimental effects on endothelial-dependent dilator responses of arteries. We used amorphous titania, which is known to be more biocompatible and less toxic than the crystalline anatase form [18]. The attenuated ACh responses induced by MSN uptake may be related to the protruding surface hydroxyl groups on MSNs reacting with intracellular H_2O_2 to produce ROS ($^\cdot$OH) as well as the generation of ROS at the nanoparticle surface. The silica nanoparticles have been shown to interact with endoplasmic reticulum NADPH (nicotinamide adenine dinucleotide phosphate reduced) oxidases, as well as activatingmembrane NADPH oxidases, which catalyses the production of superoxide anion [34; 35]. Herein, we demonstrate that MSNs generate significantly less ROS than dense SiNPs. Furthermore, MSNs have been shown to be intrinsically less toxic than nonporous SiNPs where surface coating has further been shown to improve their biocompatibility [35]. Therefore, the production of intracellular and extracellular ROS by MSNs can reduce vasodilator capacity, through quenching the naturally occurring vasodilator molecule nitric oxide. Exposure of vessels to MSNs coated with titania prevented their attenuated effects and significantly improved the endothelial dependent dilator responses. We suggest that this may be due to the reduced amount of ROS being generated by the surface of MSNs after titania coating once they are taken up into the vessel wall. Polyhydroxylated compounds are readily oxidised by holes scavengers contained within TiO_2. The scavenging efficiency is known to increase in accordance to anchoring hydroxyl groups [32]. Our findings demonstrate that while there was a highly significant reduction in fluorescence levels by MSNs in comparison to solid non-porous SiNPs, this was not significantly altered after titania coating. We measured relative fluorescence levels in solution using the DCF assay which cannot be used as a direct measure of hydrogen peroxide and other ROS moieties [36; 37]. It remains plausible, therefore, that titania coating may scavenge a range of ROS moieties, including superoxide anion, as well as reduce the capacity of the MSNs to activate NADPH oxidases within the cells [32]. The phenomenon of reduced oxidative stress induced by nanoparticles of various material composition such as ceria has also been previously

demonstrated by scavenging superoxide anions [3]. For example, an intrinsic peroxidase-like activity of superparamagnetic iron oxide nanoparticles has been shown to induce proliferation of mesenchymal stem cells as well as the acceleration of the cell cycle process by the removal of intracellular H_2O_2 [38]. This phenomenon might have been implicated in this current study favouring the protective role of the titania coating of MSNs in reducing oxidative stress. Uptake of MSNs and TiMSNs by aortic vessels had no overall effect on endothelial independent dilator responses, indicating that smooth muscle cell sensitivity to nitric oxide was unaffected by uptake.

While our study has examined the uptake and vasodilator effects of SNP-loaded TiMSNs by isolated aortic vessels under static conditions, *ex vivo*, we have previously demonstrated that SiNPs (of similar diameter) are rapidly taken up by ECs lining the vasculature in isolated vessels (under both static and flow conditions), and also *in vivo*, after intravenous administration [5]. No uptake was evident when SiNPs were added to vessels at 4 °C [12]. Our TEM images suggest that the MSNs were taken up actively by endocytosis into the vessel. These MSNs thus have the potential of being surface tagged to target ECs and hence can be used for localised delivery, *in vivo*.

5. Conclusions

Using an *ex vivo* model of vascular function, we demonstrate that titania coated MSNs enable a slow and sustained release of the SNP vasodilator drug. In addition, we demonstrate that while the MSNs offer efficient drug loading due to their high degree of porosity, the use of amorphous titania to coat their surface, significantly improves their biocompatibility and prevents detrimental effects on vessel dilator function than uncoated MSNs. These features and the increased penetrability into the vessel wall make titania coated MSNs an attractive drug delivery modality for the treatment of vascular disease.

ETHICAL CONDUCT OF RESEARCH

The authors state that they have obtained appropriate institutional review board approval and have followed the principles outlined in the Declaration of Helsinki for the animal experimental investigations.

REFERENCES

1. E.J. Benjamin and writing group members. Heart disease and stroke statistics-2017 update. A report from the American Heart Association. Circulation 135 (2017) e146-e603.

2. Y. Matsuzawa, M.D. Lerman. Endothelial Dysfunction and Coronary Artery Disease: Assessment, Prognosis and Treatment. Coron Artery Dis 25 (2014) 713-724.

3. P.M. Vanhoutte, H. Shimokawa, E.H.C. Tang, M. Feletou. Endothelial dysfunction and vascular disease. Acta Physiologica 196 (2009) 193-222.

4. F. Bossetti, ZS. Galis, MS. Bynoe, M. Charlette, MJ. Cipolla, G. del Zoppo, TS. Hatsukami, T. L. Z. Jones, J. I. Koenig, G. A. Lutty, C. Maric-Bilkan, T. Stevens, H. E. Tolunay, W. Koroshetz. Small blood vessels: Big health problems? Scientific recommendations of the national institutes of health workshop. J Am Heat Assoc. 5 (2016) e004389.

5. A. Shukur, D. Whitehead, A. Seifalian, M. Azzawi. The influence of silica nanoparticles on small mesenteric arterial function. Nanomedicine 11 (2016) 2131-46.

6. A. Farooq, T. Mohamed, D. Whitehead, M. Azzawi. Improved vasodilator responses after infusion of ceria coated silica nanoparticles, ex vivo. J Nanomedicine and Nanotechnol, 5 (2014) 195-201.

7. A. Farooq, D. Whitehead, M. Azzawi. Real-time observation of aortic vessel dilation through delivery of sodium nitroprusside by mesoporous silica nanoparticles. Journal of Colloid and interface science 478 (2016) 127-35.

8. Y.Song, Y. Li, Q. Xu, Z. Liu. Mesoporus silica nanoparticles for stimuli responsive controlled drug release: advances, challenges and outlook. Int J Nanomedicine 12 (2017) 87-110.

9. X-J. Luo, H-Y Yang, L-N Niu, J. Mao, C. Juang, DH. Pashely, FR. Tay. Translation of a solution based biomineralisaion concept into a carrier-based delivery system via the use of expanded-pore mesoporous silica. Acta Biomaterialia 31 (2016) 378–387.

10. M. Vallet-Regi, F. Balas, D. Arcos. Mesoporous materials for drug delivery. Angewandte Chemie International Edition, 46 (2007) 7548-7558.

11. Z. Tao, BB. Toms, J. Goodisman, T. Asefa. Mesoporosity and functional group dependent endocytosis and cytotoxicity of silica nanomaterials. Chemical Research in Toxicology, 22 (2009) 1869-1880.

12. N. Akbar, T. Mohamed, D. Whitehead, M. Azzawi. Biocompatibility of amorphous silica nanoparticles: Size and charge effect on vascular function, in vitro. Biotechnol. Appl. Biochem. 58 (2011) 353-362.

13. A. Farooq, D. Whitehead, M. Azzawi. Attenuation of endothelial-dependent vasodilator responses, induced by dye-encapsulated silica nanoparticles, in aortic vessels, Nanomedicine 0 (2013) 1-12.

14. T. Xia, M. Kovochich, J. Brant, M. Hotze, F.J. Semp, T. Oberley, C. Sioutas, JI. Yeh, MR. Wiesner, AE. Nel . Comparison of the abilities of ambient and manufactured nanoparticles to induce cellular toxicity according to anoxidative stress paradigm. NanoLett 6 (2006) 1794e807.

15. E.G. Seebauer, K. Dev, MYL. Jung, R. Vaidyanathan, CTM. Kwok, JW. Ager, EE. Haller, RD. Braatz, Control of defect concentrations within a semiconductor through adsorption. Phys. Rev. Lett. 97 (2006) 055503.

16. N.M. Jukapli, S. Bagheri. Recent developments on titania nanoparticle as photocatalytic cancer cells treatment. J Photochem Photobiol B. 163 (2016) 421-30.

17. T. Close, G. Tulsyan, C.A. Diaz, SJ. Weinstein, C. Richter. Reversible oxygen scavenging at room temperature using electrochemically reduced titanium oxide nanotubes, Nature Nanotechnology 10 (2015) 418-422.

18. K.C.W. Wu, Y. Yamauchi, C.Y. Hong, Y.H Yang, Y.H. Liang, T. Funatsu, M. Tsunoda. Biocompatible, surface functionalized mesoporous titania nanoparticles for intracellular imaging and anticancer drug delivery. Chemical Communications, 47 (2011) 5232-5234.

19. I. Slowing, B.G. Trewyn, V.S.-Y. Lin, Effect of surface functionalization of MCM-41-type mesoporous silica nanoparticles on the endocytosis by human cancer cells, JACS 128 (2006) 14792-14793.

20. P.J. Kelly, R.D. Arnell, 'Magnetron sputtering: A review of recent developments and applications.' *Vacuum,* 56 (2000) 159-172.

21. M. Ratova, P.J. Kelly, G.T. West, L. Tosheva, M. Edge. Reactive magnetron sputtering deposition of bismuth tungstate onto titania nanoparticles for enhancing visible light photocatalytic activity. Applied Surface Science, 392 (2017) 590-597.

22. P.J. Kelly, G.T. West, M. Ratova, L. Fisher, S. Ostovarpour, J. Verran, 'Structural formation and photocatalytic activity of magnetron sputtered titania and doped-titania coatings', *Molecules,* 19 (2014) 16327-16348.

23. W. Lin, Y.W. Huang, X.D. Zhou, Y. Ma. In vitro toxicity of silica nanoparticles in human lung cancer cells. Toxicology and applied pharmacology, 217 (2006) 252-259.

24. S. Dash, P.N. Murthy, L. Nath, P. Chowdhury. Kinetic modelling on drug release from controlled drug delivery systems. Acta Pol Pharm, 67 (2010) 217-23.

25. N.A. Peppas. Analysis of fickian and non-fickian drug releasefrom polymers. Pharm. Acta Helv. 60 (1985) 110–111.

26. F. Rehman, P.L. Volpe, C. Airoldi. The applicability of ordered mesoporous SBA-15 and its hydrophobic glutaraldehyde-bridge derivative to improve ibuprofen-loading in releasing system. Colloids and Surfaces B: Biointerfaces, 119 (2014) 82-89.

27. J. Siepmann, N.A. Peppas. Modeling of drug release from delivery systems based on hydroxypropyl methylcellulose (HPMC). Adv Drug Deliv Rev. 48 (2001)139–57.

28. A. Vakurov, R. Drummond-Brydson, O. Ugwumsinachi, A. Nelson. Significance of particle size and charge capacity in TiO2 nanoparticle lipid interactions. J colloid and interface Science 473 (2016) 75-83.

29. E. Wahlström, E.K. Vestergaard, R. Schaub, A. Rønnau, M. Vestergaard, E. Lægsgaard, I. Stensgaard, F. Besenbacher. Electron transfer-induced dynamics of oxygen molecules on the TiO_2(110) surface. Science 303 (2004) 511–513.

30. G. Pacchioni. Oxygen vacancy: the invisible agent on oxide surfaces. ChemPhysChem 4, (2003) 1041–1047.

31. C.B. Gopala, S.M. Hailem. An electrical conductivity relaxation study of oxygen transport in samarium doped ceria. J. Mater. Chem. A. 2 (2014) 2405–2417.

32. I.A. Shkrob, M.C. Jr Sauer, D. Gosztola. Efficient, Rapid Photo-oxidation of Chemisorbed Polyhydroxyl Alcohols and Carbohydrates by TiO2 Nanoparticles in an Aqueous Solution, Journal of Physical Chemistry B, 108 (2004) 12512–12517.

33. S.R. Saptarshi , A. Duschl, A.L. Lopata. Interaction of nanoparticles with proteins: relation to bio-reactivity of the nanoparticle. J Nanobiotechnol 11 (2013) 26-32.

34. S.N.P. Voicu, D. Dinu, C. Sima, A. Hermenean, A. Ardelean, E. Codrici, M.S. Stan, O. Z˜arnescu, A. Dinischiotu. Silica Nanoparticles Induce Oxidative Stress and Autophagy but Not Apoptosis in the MRC-5 Cell Line. Int. J. Mol. Sci. 16 (2015) 29398–29416.

35. S.E. Lehman, A.S. Morris, PS. Mueller, AK. Salem, VH. Grassian, SC. Larsen. Silica Nanoparticle-Generated ROS as a Predictor of Cellular Toxicity: Mechanistic Insights and Safety by Design. Environ Sci Nano. 3 (2016) 56–66.

36. B. Kalyananaman, V. Darley-Usmar, K.J.A. Davies, P.A. Dennery, H.J. Forman, M.B. Grisham, G.E. Mann, K. Moore, J. Roberts, H. Ischiropoulos. Measuring reactive oxygen and nitrogen species with fluorescent probes: challenges and limitations. Free Rad Biol Med 52 (2012) 1-6.

37. L.M. Tetz, P.W. Kamau, A.A. Cheng, J.D. Meeker, R. Loch-Caruso. Troubleshooting the dichlorofluorescein assay to avoid artifacts in measurement of toxicant-stimulated cellular production of reactive oxidant species. J Pharmacol Toxicol Methods 67 (2013) 56-60.

38. DM. Huang, JK. Hsiao, YC. Chen, LY. Chien, M. Yao, YK. Chen, C.S. Yang, YC. Chen. The promotion of human mesenchymal stem cell proliferation by superparamagnetic iron oxide nanoparticles. Biomaterials 30 (2009) 3645-51.

FIGURE CAPTIONS

Figure 1: Mesoporous silica nanoparticle characterisation. SEM images of A) MSN, B) MSN-SNP, C) TiMSN and D) TiMSN-SNP. TEM images of E) MSN, and F) TiMSN. EDS analysis confirms the presence of silica (G) and titanium (D) for MSNs and TiMSNs, respectively.

Figure 2: Chemical analysis of the synthesized mesoporous silica nanoparticles. A) XRD patterns of the samples of MSN (blue line) and TiMSN (red line), A and R represent the position of anatase and rutile peaks, respectively. B) ATR spectra of MSN and MSN template extracted. C) Nitrogen adsorption-desorption isotherms of MSN, TiMSN and corresponding SNP-loaded samples. Close symbols, adsorption; open symbols, desorption. The inset shows corresponding pore-size distributions. D) DCF assay assessment of the relative fluorescence generated by the nanoparticles; *p<0.001; error bars=standard error of mean.

Figure 3: Drug release by the mesoporous silica nanoparticles. A) Percent release profile of sodium nitroprusside from mesoporous nanoparticles using atomic absorption spectroscopy. Drug release kinetic models of MSN-SNP and TiMSN-SNP in PBS B) First order, C) Higuchi and D) Koresmeyer–Peppas.

Figure 4: The influence of nanoparticle uptake on aortic vessel dilation. TEM microscopy images of sections from fixed aortic vessels after a 10 min incubation period with A) MSN showing uptake within an endothelial cell and B) TiMSN showing uptake within an endothelial cell C) TiMSN within smooth muscle cells and D) TiMSN in elastic lamina. E) Timecourse of aortic vessel dilation in response to uptake of sodium nitroprusside loaded mesoporous nanoparticles. 'n' is number of vessels. error bars=standard error of mean. The influence of both MSN and TiMSN on endothelium-dependent (F) and independent (G) vasodilator

responses. The control is incubation in PSS alone. 'n' is number of vessels. *=p<0.05,

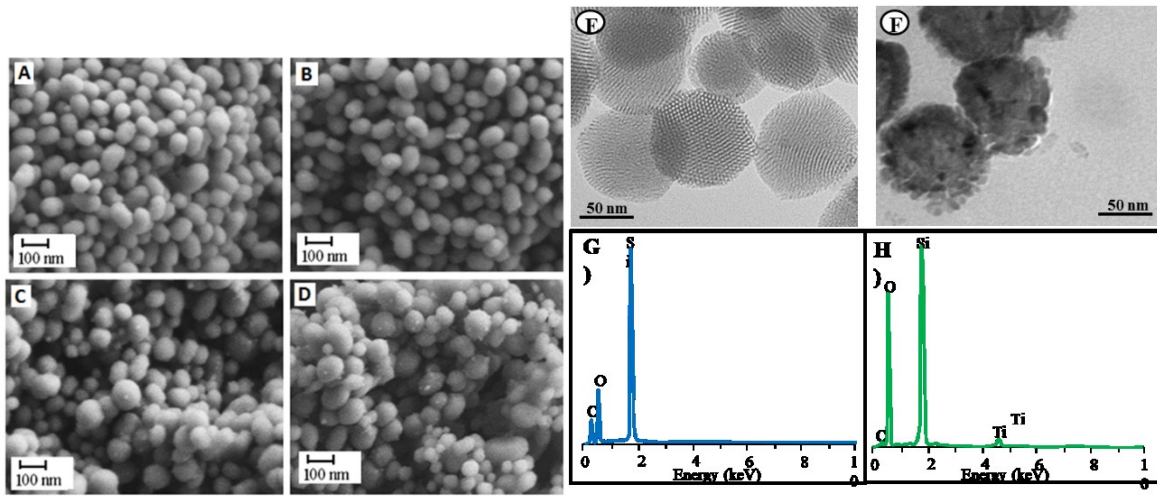**=p<0.01 #=p<0.001, error bars=standard error of mean.
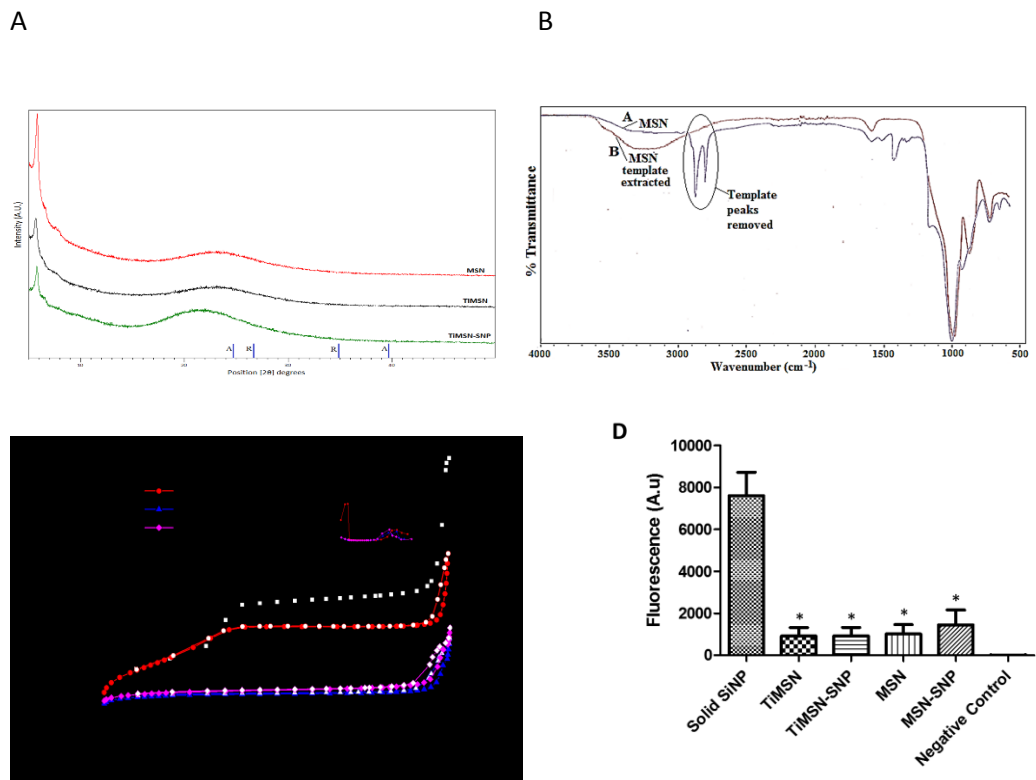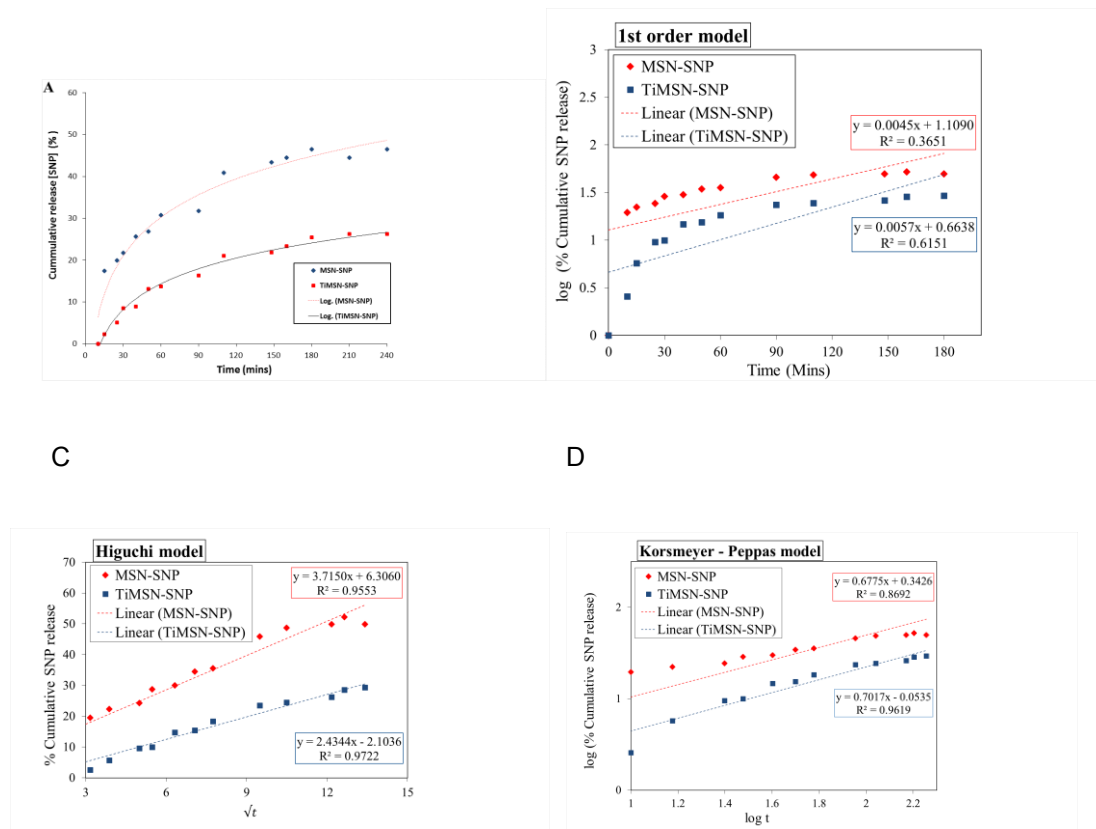
Figure 1

Figure 2

A

B

D

Figure 3

Figure 4